Poklar, N., Lah, J., Salobir, M., Macek, P. & Vesnaver, G. pH and temperature-induced molten globule-like denatured states of equinatoxin II: a study by UV-melting, DSC, far- and n...

ARTICLE *in* BIOCHEMISTRY · DECEMBER 1997

Impact Factor: 3.02 · DOI: 10.1021/bi971719v · Source: PubMed

5 AUTHORS, INCLUDING:

Nataša Poklar Ulrih
University of Ljubljana
120 PUBLICATIONS **1,506** CITATIONS
SEE PROFILE

Jurij Lah
University of Ljubljana
45 PUBLICATIONS **907** CITATIONS
SEE PROFILE

Peter Maček
University of Ljubljana
124 PUBLICATIONS **4,072** CITATIONS
SEE PROFILE

Gorazd Vesnaver
University of Ljubljana
67 PUBLICATIONS **1,381** CITATIONS
SEE PROFILE

pH and Temperature-Induced Molten Globule-Like Denatured States of Equinatoxin II: A Study by UV-Melting, DSC, Far- and Near-UV CD Spectroscopy, and ANS Fluorescence†

Nataša Poklar,‡ Jurij Lah,‡ Mateja Salobir,‡ Peter Maček,§ and Gorazd Vesnaver*,‡

Department of Chemistry, University of Ljubljana, Ljubljana, Slovenia, and Department of Biology, Biotechnical Faculty, University of Ljubljana, Ljubljana, Slovenia

Received July 14, 1997; Revised Manuscript Received September 5, 1997⊗

ABSTRACT: Thermal denaturation of equinatoxin II (EqTxII) in glycine buffer solutions (pH 1.1, 2.0, 3.0, and 3.5) and in triple distilled water (pH 5.5−6.0) was examined by differential scanning calorimetry, UV and CD spectroscopy and fluorescence emission spectroscopy of the added hydrophobic fluorescent probe ANS. At pH 5.5−6.0 and at temperatures below 60 °C, the protein exists in a native state characterized by a pronounced tertiary structure, a β-rich secondary structure and a low degree of ANS-binding. At higher temperatures, it undergoes a two-state conformational transition, $(\Delta H°)_{VH} = (\Delta H°)_{DSC}$, into an unfolded state, which is characterized by a complete collapse of its tertiary structure and an incomplete denaturation of its secondary structure. At acidic pH, the EqTxII temperature-induced conformational transition appears at lower temperatures as non-two-state transition accompanied by the formation of an intermediate state which shows characteristics of molten globules, i.e., absence of defined tertiary structure, increase in α-rich secondary structure, and high affinity for ANS. At pH 2.0, the low-temperature initial state of EqTxII is already partially denatured; the tertiary structure is partially disrupted, and a pronounced inequality $(\Delta H°)_{VH} > (\Delta H°)_{DSC}$ is observed. At pH value of 1.1 and below 60 °C, EqTxII exists in a stable acid-denatured compact state which shows all the characteristics of a molten globule, which even at 95 °C is not completely denatured. According to numerous studies on the pore forming toxins, such acid-denatured compact states may contribute to the protein's ability to penetrate into biological membranes.

Recent in vitro studies of unfolding of some globular proteins have indicated that various non-native protein states may be involved in physiological processes such as protein penetration into biological membranes *(1)* or ligand delivery to target cells via transport proteins *(2)*. Studies on pore forming toxins have shown that penetration of these proteins into membranes is associated with significant conformational changes *(3, 4)*. These changes may also be induced by lowering the pH and involve the partial denaturation of the proteins into intermediates which have a well-preserved secondary structure and no or almost no tertiary structure and are relatively compact. Such intermediates are commonly called molten globule states *(5−7)*. Although a detailed mechanism of protein penetration into membranes remains unknown, evidence has accumulated indicating that a local acidic pH near the negatively charged membrane surfaces provokes a partial denaturation of protein molecules thus enabling penetration into the membranes *(8−10)*.

Equinatoxin II (EqTxII)[1] is a globular protein that exhibits an ability to bind to natural or model lipid membranes and form pores selective to cations *(11)*. It consists of 179 amino acid residues (M = 19.8 kDa). Our recent investigation of pH-induced conformational transitions of EqTxII monitored by measuring its intrinsic fluorescence and the fluorescence of added hydrophobic fluorescent probe ANS (1-anilino naphthalene-8-sulfonic acid ammonium salt) has shown that EqTxII exhibits the highest stability in pure aqueous solutions (pH 5.5−6.0) while at low pH it shows some characteristics of a compact acid-denatured state *(12)*. Several studies performed on other pore-forming proteins have indicated that loosening of their tertiary structure induced by lowering pH leads to an enhanced membrane penetration *(4, 13, 14)*. To see if such pH-induced partial denaturation has a similar effect on the pore forming ability of EqTxII molecules, one should first provide a reliable structural description of intermediate states formed at the acidic unfolding of the protein. In other words, prior to studying the EqTxII membrane penetrating ability, one should investigate its unfolding equilibria, identify and characterize the intermediates between its native and denatured states, and estimate their relative population.

The present work was aimed at learning more about the native and low-pH conformations of EqTxII with a hope of extending our understanding of the protein unfolding pathways involved in the process of its insertion into membranes. Thermally induced conformational transitions of EqTxII in solutions of varying pH were investigated by UV spectroscopy, DSC, far- and near-UV CD spectroscopy, and fluorescence of the added fluorescent probe, ANS. The results

† This work was supported by the Ministry of Science and Technology of the Republic of Slovenia.

* To whom correspondence should be addressed. Department of Chemistry, University of Ljubljana, Aškerčeva 5, 1000 Ljubljana, Slovenia. Fax: +38661 1254458. E-mail: gorazd.vesnaver@uni-lj.si.

‡ Department of Chemistry.

§ Department of Biology.

⊗ Abstract published in *Advance ACS Abstracts,* November 1, 1997.

[1] Abbreviations: ANS, 1-anilino naphthalene-8-sulfonic acid ammonium salt; EqTxII, equinatoxin II; Gu-HCl, guanidine hydrochloride.

S0006-2960(97)01719-4 CCC: $14.00

provide strong evidence that at low pH values or high temperatures EqTxII exists in a molten globule state characterized by a well-pronounced non-native α-rich secondary structure, a complete absence of tertiary structure, and a high affinity for ANS.

MATERIALS AND METHODS

Materials. EqTxII was isolated from the sea anemone *Actinia equina* L. *(15)*, stored as a powder at −10 °C, and used without any further purification. Protein solutions for UV spectroscopy ($c = 0.14$ mg/$g_{solution}$) and fluorescence ($c = 0.05$ mg/$g_{solution}$) measurements were prepared daily from defrozen aqueous stock solutions by diluting them into either triple distilled water, 0.1 M glycine buffers of appropriate pH or in 6 M Gu-HCl. The external fluorescence probe ANS (1-anilino naphthalene-8-sulfonic acid ammonium salt) was a product of Fluka (Buchs, Switzerland) and was used without any additional purification. More concentrated ($c \approx 1$ mg/$g_{solution}$) EqTxII solutions for the CD measurements in the far- and near-UV range and for the DSC measurements were prepared directly by dissolving the protein in the appropriate solvent.

UV Spectrophotometry. UV absorbance measurements were performed in a Cary 1 UV−visible spectrophotometer (Varian, Australia) using matched 1 cm path length quartz cuvettes. The spectrophotometer was equipped with an electrothermal temperature controller which provides thermal programmability for the multiple cell unit so that the absorbance measurements can be performed directly as a function of temperature. Equilibrium thermal unfolding of EqTxII was monitored by recording absorbance at 232 nm as a function of temperature over the appropriate temperature range (in most cases 20−90 °C). The wavelength 232 nm was chosen because of the maximal difference between the denatured and the native protein spectra observed at this wavelength. The heating rate was 0.5 °C min^{-1}.

Circular Dichroism (CD) Spectropolarimetry. CD experiments were performed on an AVIV Model 62A DS Spectropolarimeter (Aviv Associates, Lakewood, NJ) equipped with a thermoelectrically controlled cell holder. CD spectra of EqTxII were measured in the far-UV range (200−250 nm) in 1 mm path length quartz cuvettes and in the near-UV range (250−300 nm) in 10 mm path length quartz cuvettes. Spectra were measured at 5 °C intervals in the temperature range from 0 to 95 °C with an averaging time of 3 s, an equilibration time of 3 min, and a band width of 1 nm. The mean residue ellipticity, [Θ], was calculated by using the relation

$$[\Theta]_\lambda = \frac{\mathrm{Mo}\Theta_\lambda}{100cl} \qquad (1)$$

in which Mo is the mean residue molar mass, Θ_λ is the measured ellipticity in degrees, c is the concentration in grams per milliliter, and l is the path length in decimeters. The value of Mo = 110.6 g/mol was obtained from MW of EqTxII (19.8 kDa) by dividing it with the number of aminoacid residues (179) constituting the EqTxII molecule. $[\Theta]_\lambda$ was expressed in degrees squared centimeters per decimole.

ANS Fluorescence Measurements. All emission fluorescence measurements were performed in a Perkin-Elmer Model LS-50 Luminescence spectrometer with a water thermostated cell holder using a 1 cm path length quartz cuvette. Slit widths with a nominal band-pass of 5 nm were used for both excitation and emission beams. An excitation wavelength of 365 nm was used, and the ANS emission spectra were recorded in the range from 380 to 600 nm. The temperature range in which all the spectra were taken at 5 °C intervals was from 3 to 83 °C, and the scan rate was 250 nm/min. The temperature in the cell was measured with an Fe/Fe-constantan thermocouple. Changes of the ANS emission spectra induced by the EqTxII conformational changes were followed by measuring the emission intensity at 483 nm at constant concentrations of EqTxII (0.05 mg/$g_{solution}$) and ANS (0.126 mg/$g_{solution}$) at which the protein was always saturated with the bound ANS *(12)*. Measuring the ANS fluorescence (bis-ANS) to follow the intermediate states of another globular protein, DnaK, at higher temperatures had been successfully used before *(16)*.

Differential Scanning Calorimetry. DSC experiments were performed in a micro-DSC Calorimeter from Setaram (Caluire, France) described elsewhere *(17)*. The sample and the reference cells of optimal operational volume of 0.8 mL were used. Calibration was performed with special cells using the Joule effect. Thermograms of EqTxII solutions in triple distilled water (pH 5.5−6.0) and in 0.1 M glycine buffers with pH 3.5, 3.0, and 2.0 were recorded over the temperature range between 20 and 80 °C at a heating rate of 0.5 °C min^{-1}. The base lines obtained by vessels filled with equal quantities of solvent were subtracted from the thermograms of protein solutions to obtain the typical corrected thermograms.

RESULTS AND DISCUSSION

UV Spectroscopy. Comparison of the absorbance spectra of EqTxII in its native (triple distilled water; pH 5.5−6.0 at room temperature) and denatured (thermal or chemical denaturation) form revealed major changes in absorbance at wavelengths around 230 nm and not in the 270−300 nm wavelength region where characteristic peaks in absorption spectra of tyrosine and tryptophane residues occur *(18, 19)*. As shown by Donovan *(20)*, spectral changes occurring in the 230 nm region result primarily from changes in the environment of the aromatic chromophores indole and phenol and are proportional to the absorbance changes observed near 280 nm. This notion is consistent with our results which have shown that the values of thermodynamic quantities describing the process of EqTxII thermal unfolding determined from melting curves at 232 nm ($c = 0.14$ mg/$g_{solution}$) and at 293 nm ($c = 0.43$ mg/$g_{solution}$) coincide within the experimental error. As a consequence of these findings, most of the UV-melting curves were measured at 232 nm (Figure 1).

Assuming the EqTxII thermal unfolding to be a two-state transition, the standard apparent or van't Hoff enthalpy of unfolding, $(\Delta H^\circ_{VH})_{UV}$, was determined from the slope of the E vs T curve at the temperature of the half-transition, T_d^{UV}, using the relation *(21)*

$$(\Delta H^\circ_{VH})_{UV} = 4R(T_d^{UV})^2\left(\frac{\delta f_D}{\delta T}\right)_{T=T_d{}^{UV}} \qquad (2)$$

in which f_D is the degree of the protein denaturation,

Table 1: Thermodynamic Characteristics of EqTxII Denaturation at Different pH Obtained by UV Spectroscopy, DSC, and Near-UV CD Spectroscopy

pH	[a]UV T_d^{UV} (K)	[a]DSC T_d^{DSC} (K)	[a]near-UV CD T_d^{CD} (K)	[b]UV $(\Delta H^\circ_{VH})_{UV}$ (kJ mol^{-1})	[b]DSC $(\Delta H^\circ_{VH})_{DSC}$ (kJ mol^{-1})	[c]DSC $(\Delta H^\circ)_{DSC}$ (kJ mol^{-1})	[b]near-UV CD $(\Delta H^\circ_{VH})_{CD}$ (kJ mol^{-1})
2.0	313.1	317.6	311.5	293	240	117	264
3.0	325.5	328.1	324.6	363	380	310	370
3.5	332.2	335.1	332.5	402	403	371	350
5.5−6.0	338.6	339.0	339.2	441	430	441	433

[a] Estimated relative error = ±0.1%. [b] Estimated relative error = ±10%. [c] Estimated relative error = ±10−20%.

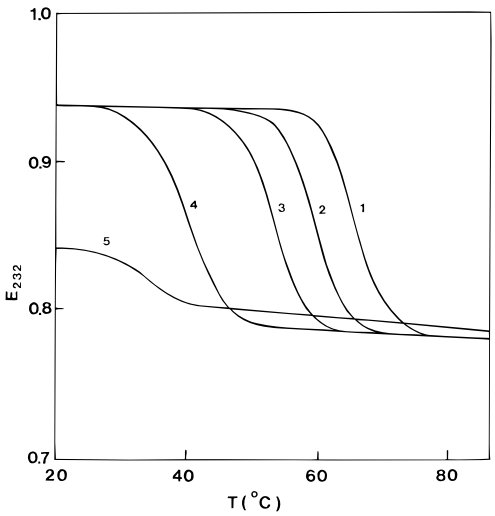

FIGURE 1: Absorbance of EqTxII at 232 nm, E_{232}, as a function of temperature in triple distilled water at pH 5.5−6.0 (1) and glycine buffers at pH 3.5 (2), 3.0 (3), 2.0 (4), and 1.1 (5); c = 0.14 mg/$g_{solution}$.

expressed in terms of the measured absorbance, E, as

$$f_D = \frac{E(T) - E_N(T)}{E_D(T) - E_N(T)} \quad (3)$$

where N and D refer to the native and denatured state, respectively. The derivative $(\delta f_D/\delta T)_{Td}$ in eq 2 can be approximated with the reciprocal value of the width of the temperature interval ΔT in which the transition is completed, and the van't Hoff equation then simplifies to

$$(\Delta H^\circ_{VH})_{UV} = 4R(T_d^{UV})^2 \frac{1}{\Delta T} \quad (4)$$

The calculated values of $(\Delta H^\circ_{VH})_{UV}$ and the corresponding values of T_d^{UV} for the thermally induced conformational transitions of EqTxII in pure water and buffers at pH ≤ 3.5 are collected in Table 1. They clearly show that EqTxII is thermodynamically most stable in pure water at pH 5.5−6.0 and that on lowering pH its stability decreases. This decreasing is manifested as a pronounced drop of T_d^{UV} and the corresponding $(\Delta H^\circ_{VH})_{UV}$ values. In solutions of higher ionic strength (buffers or simple salt added) and pH above 3.5, EqTxII tended to aggregate already at low temperatures. Therefore, its melting curves were studied only in pure aqueous solutions or in buffers with pH ≤ 3.5. The reversibility of denaturation under the conditions employed was high (above 90%).

As can be seen from Figure 2, the values of $(\Delta H^\circ_{VH})_{UV}$ obtained in EqTxII solution of different pH increase linearly with the temperature of half-transition, T_d^{UV}. Assuming a

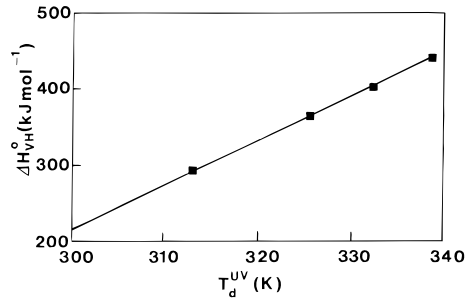

FIGURE 2: The van't Hoff enthalpy of conformational transition, $(\Delta H^\circ_{VH})_{UV}$, as a function of the temperature of the half transition, T_d^{UV}, determined from the UV-melting curves of EqTxII in solutions of pH between 2.0 and 5.5−6.0 (Table 1).

two-state transition, the slope $\delta(\Delta H^\circ_{VH})_{UV}/\delta T_d^{UV}$ coincides quantitatively with the apparent standard heat capacity difference between the denatured and native state of the protein, $(\Delta C_p^\circ)^{app}$ *(22)*. The value of $(\Delta C_p^\circ)^{app}$ determined in this manner was 5.8 kJ K^{-1} mol^{-1}.

Far- and Near-UV CD Spectroscopy. The change in secondary structure of EqTxII as a function of temperature and pH can be followed by measuring the protein's far-UV CD spectra (Figures 3−5).

In the triple distilled water (pH 5.5−6.0), EqTxII shows at temperatures below ∼70 °C the far-UV CD spectra with a minimum at 217 nm (Figure 3a) characteristic of proteins containing predominantly β-sheet structures *(23)*. We analyzed the CD spectra with a computer program CONTIN *(24, 25)* which calculates the secondary structure as a linear combination of spectra from a database of 16 proteins with known conformations including four proteins denatured to random conformation *(26)*. On the basis of this analysis, we estimated that EqTxII contains at 0 °C about 12% of α-helix, 42% of β-sheet, 15% of β-turn, and 31% of remainder structure. The calculated amount of α-helix is lower than was estimated before *(27)*.

Decreasing the pH to a value of 2.0 at temperatures between 0 and ∼40 °C has almost no effect on the EqTxII far-UV CD spectra, indicating the stability of its β-rich structure (Figure 4a). Further decreasing of pH in this temperature range, however, leads to a pronounced increase of the protein's α-helical content reflected in significant changes of its far-UV CD spectra (Figure 5a, appearance of minima at 209 and 217 nm). Using the already mentioned CD spectral analysis, we calculated that at 0 °C and pH 1.1 EqTxII contains about 18% of α-helix (50% increase), 35% of β-sheet, 12% of β-turn, and 35% of the remainder structure. Similar conformational changes were also observed when protein solutions at pH between 5.5−6.0 and 2.0 were heated from ∼(40−70) to 95 °C. As shown in Figures 3a, 4a, and 5a, the EqTxII far-UV CD spectra switch at high temperatures from a shape characteristic of proteins

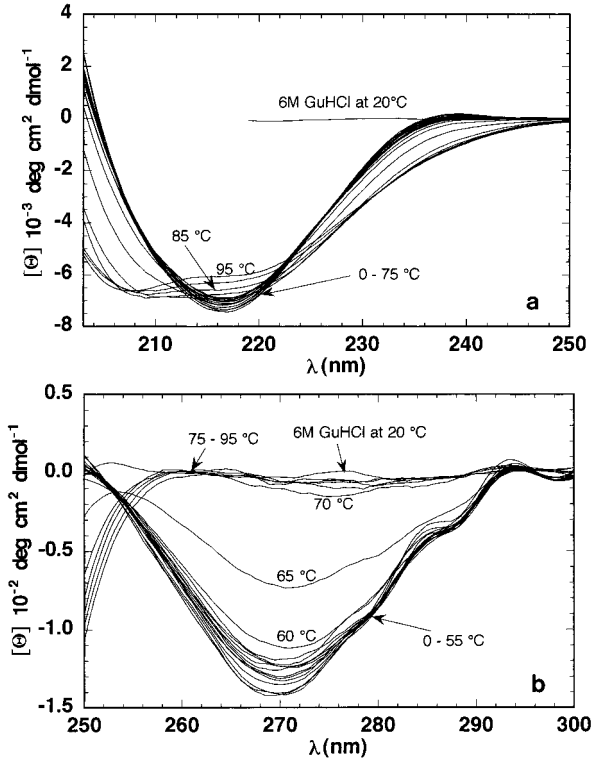

FIGURE 3: Temperature dependence of the far-UV CD spectra (panel a) and the near-UV CD spectra (panel b) of EqTxII in pure aqueous solution at pH 5.5−6.0.

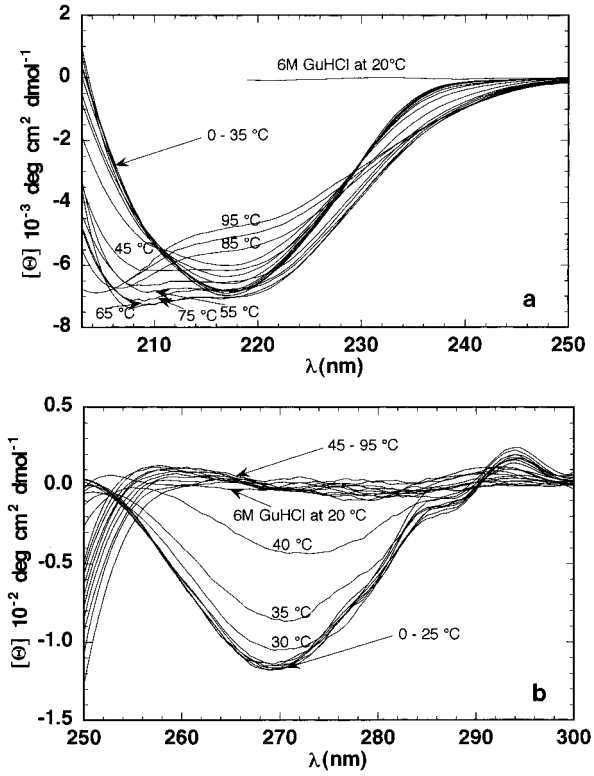

FIGURE 4: Temperature dependence of the far-UV CD spectra (panel a) and the near-UV CD spectra (panel b) of EqTxII in glycine buffer solution at pH 2.0.

with a high content of β-structures into a shape that closely resembles the one observed at pH 1.1 and low temperatures and is typical of proteins rich in α-helix structures. At pH 1.1, where α-helix-rich structure of EqTxII is observed already at 0 °C and is stable up to 60 °C, increasing of temperature above 60 °C results in further transition from

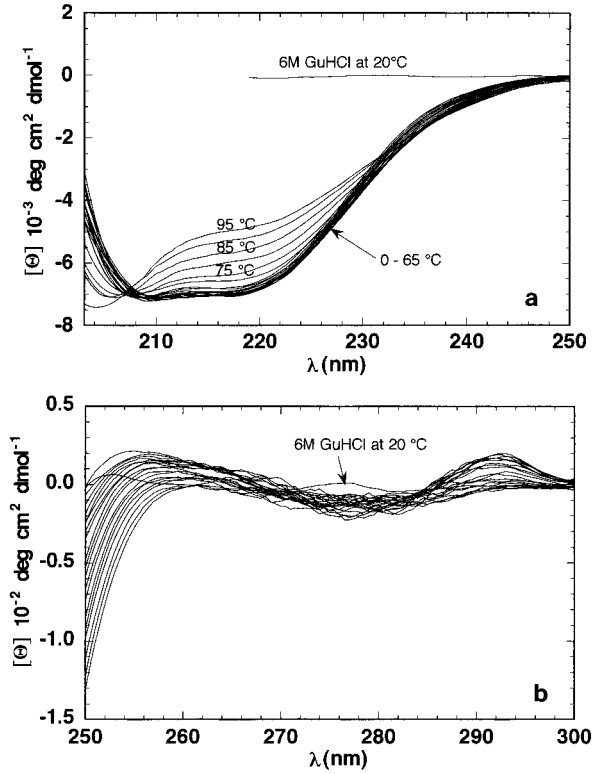

FIGURE 5: Temperature dependence of the far-UV CD spectra (panel a) and the near-UV CD spectra (panel b) of EqTxII in glycine buffer solution at pH 1.1.

α-rich into remainder-rich structures (isoelliptic point at 207 nm). Comparison with the EqTxII far-UV CD spectrum observed in 6 M Gu-HCl shows, however, that even at the lowest measured pH and the highest measured temperature, EqTxII retains secondary structure elements (Figure 5a).

Changes in the protein tertiary structure can be followed from its CD spectra in the near-UV range where the CD signals originate mainly from aromatic amino acids and cystine *(28).* In the triple distilled water (pH 5.5−6.0) below ∼60 °C, EqTxII with its five tryptophane, 11 tyrosine, and five phenylalanine residues shows a pronounced minimum at 270 nm (Figure 3b), which indicates the existence of a defined tertiary structure *(6, 7, 29).* Lowering the pH causes the extent of the tertiary structure to decrease until at pH 1.1 it disappears completely at all measured temperatures as deduced from the comparison with the corresponding CD spectrum determined in 6 M Gu-HCl (Figure 5b). Such a total collapse of the EqTxII tertiary structure is observed also at pH between 2.0 and 5.5−6.0 if the temperature of the protein solution is sufficiently increased (Figures 3b and 4b). When heated above ∼65 °C at pH 5.5−6.0, the EqTxII tertiary structure collapsed in a sharp two state manner (Figure 6d) and the transition is completed around 80 °C. Similar changes in the near-UV CD spectra of EqTxII induced by increasing the temperature were observed also at pH 3.5 (data not shown) and 3.0. In these solutions, the intensity of the minima at 270 nm occurring at low temperatures remained unchanged while the temperature-induced collapse of the protein tertiary structure was shifted to lower temperatures (Figure 6c). At pH 2.0, however, the intensity of the low-temperature minima at 270 nm in near-UV CD spectra became less pronounced (Figure 4b), suggesting that at this pH the EqTxII tertiary structure is partially disrupted already at low temperatures. In the

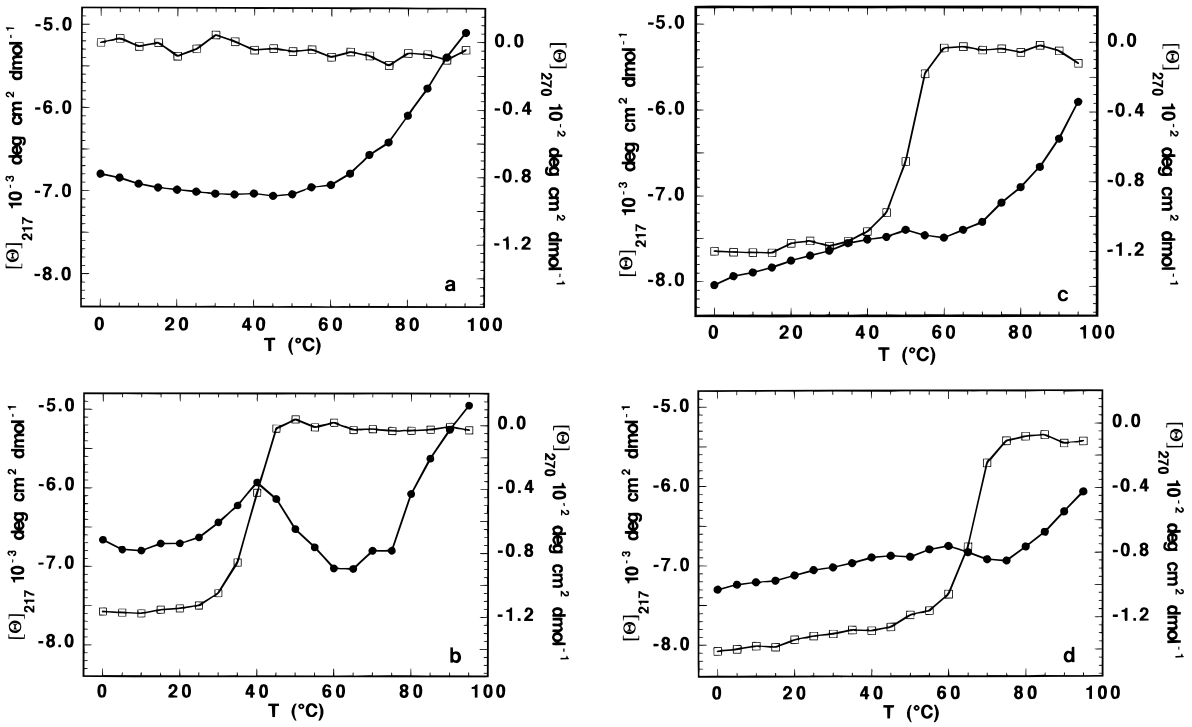

FIGURE 6: Far- (●) and near- (□) UV CD melting curves of EqTxII in glycine buffers at pH 1.1 (panel a), pH 2.0 (panel b), pH 3.0 (panel c), and in the triple distilled water at pH 5.5−6.0 (panel d); [Θ] is given in degree squared centimeters per decimole.

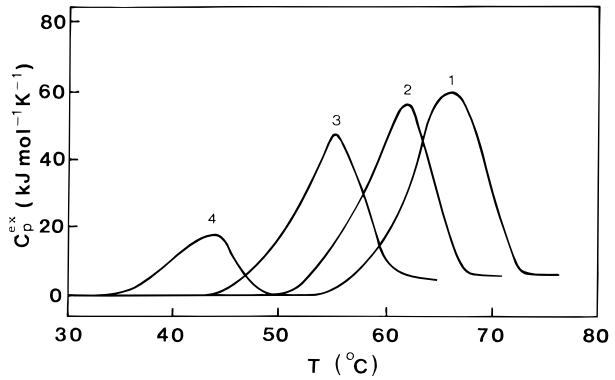

FIGURE 7: Corrected DSC thermograms of EqTxII in pure aqueous solution at pH 5.5−6.0 (1) and in glycine buffers at pH 3.5 (2), 3.0 (3), and 2.0 (4); c = 1.2 mg/$g_{solution}$.

temperature range for which the UV (Figure 1) and DSC melting curves (Figure 7) have shown characteristic conformational transitions, the corresponding CD melting curves (Figure 6) show only disruption of tertiary structure while the secondary structure remains more or less unchanged. Assuming that the observed collapse of the EqTxII tertiary structures can be described as a two-state process, we determined the corresponding van't Hoff enthalpies of transition. Using the same procedure as with UV melting curves (eqs 2−4), we obtained $(\Delta H^{\circ}_{VH})_{CD}$ values from the near-UV CD melting curves presented in Figure 6. They agree well with the corresponding van't Hoff enthalpies obtained from UV and DSC measurements (Table 1), suggesting that the three methods applied here monitor the same conformational transition of EqTxII.

Analysis of the measured CD spectra clearly shows that the equilibrium unfolding of EqTxII induced by lowering pH or increasing the temperature is accompanied by a formation of thermodynamically stable intermediates with only secondary structure and no tertiary structure which, therefore, may be classified as molten globule states *(5−7, 30)*. As can be seen from Figures 3a, 4a, and 5a, the intermediates exhibit far-UV CD spectra more typical of α-helical conformations, in contrast to the toxin native state rich in *β*-structures.

Recent studies of conformational transitions of numerous proteins at high temperatures, in denaturant solutions, or at low pH have shown that different proteins may undergo transitions through different intermediate states depending on the protein architecture and on the agent inducing its conformational transition. In their investigation of the membrane insertion of the pore forming domain of colicin A, van der Goot et al. *(1)* have shown that at 25 °C this pore forming domain undergoes a native to molten globule transition at acidic pH. From the far- and near-UV CD spectra, they concluded that below pH 4 the colicin A pore-forming fragment adopts the features of the molten globule state with a rather compact and well-pronounced secondary structure but no rigid tertiary structure. They have suggested that such intermediate states provide the best pathway for making a protein structure competent for a penetration into membranes. Similar results have been reported on another pore-forming protein, diphtheria toxin, for which it has been shown that its low-pH and high-temperature conformations are closely related. They both appear as partially denatured states which, according to their intrinsic fluorescence and far- and near-UV CD spectra, contain only a considerable secondary structure *(3)*. Furthermore, by applying molecular dynamics simulation to investigate the acid and thermal denaturation of barnase, Caflisch and Karplus *(31)* have shown that the unfolding behavior of the protein at low pH/low temperatures closely resembles the one observed at neutral pH/high temperatures. Recently, Chalikian et al. *(32)* have constructed a phase diagram characterizing conformational transition of α-chymotrypsinogen A (α-ctg A) as a function of pH and temperature. They found that below pH

3.1 the heat-induced denatured state of α-ctg A is molten globule, lacking the native-like tertiary structure, while exhibiting significant amounts of secondary structure. Finally, our observation of an accumulation of α-helical intermediates during the unfolding of EqTxII is supported by the results of similar study performed on β-lactoglobulin, a predominantly β-sheet protein. In the recent study of refolding kinetics of the β-lactoglobulin, Hamada et al. *(33)* have reported that the folding of this protein follows a nonhierarchical pathway characterized by folding intermediates that contain non-native α-helical structures.

DSC. It is well-known that calorimetric measurements provide a direct, model-independent determination of transition enthalpies. A result of such a measurement, obtained after the baseline subtraction, is a so-called thermogram characterized by a peak centered at the temperature T_d^{DSC} at which the ratio between the native and denatured form of the protein is supposed to be 1:1. The area under such curve is proportional to the enthalpy of denaturation at T_d^{DSC}, $(\Delta H_d)_{DSC}$, and assuming that this enthalpy does not depend on the protein concentration, the measured $(\Delta H_d)_{DSC}$ equals the standard enthalpy of denaturation, $(\Delta H_d^\circ)_{DSC}$. Analysis of DSC-thermograms also leads to a model-dependent van't Hoff standard enthalpy of conformational transition, $(\Delta H_{VH}^\circ)_{DSC}$, expressed for a two-state model as *(22)*

$$(\Delta H_{VH}^\circ)_{DSC} = 2T_d^{DSC}\sqrt{R(\Delta c_p)_{T_d} M_2} \qquad (5)$$

where M_2 is the protein molecular weight and $(\Delta c_P)_{T_d}$ is the difference between the measured specific heat capacity of the protein at T_d^{DSC} and the average value of the specific heat capacities of the native and denatured protein extrapolated to the T_d^{DSC}.

Corrected thermograms of EqTxII in pure aqueous solution and in glycine buffers with pH 3.5, 3.0, and 2.0 are shown in Figure 7. The calorimetric scan of EqTxII in pure water is characterized by a single peak centered at about 66 °C, which, with increased acidity, shifts to lower temperatures and becomes less pronounced. At pH <2.0, the peak becomes to low for a reliable determination of the measured heat effects. The values of T_d^{DSC}, $(\Delta H_d^\circ)_{DSC}$, and $(\Delta H_{VH}^\circ)_{DSC}$ for the EqTxII solutions in triple-distilled water (pH 5.5−6.0) and in glycine buffers with pH 3.5, 3.0, and 2.0 are collected in Table 1. The T_d^{DSC} and $(\Delta H_{VH}^\circ)_{DSC}$ values are in good agreement with the corresponding values obtained from the UV and CD-melting curves which means that by monitoring the absorbance at 232 nm and ellipticity at 270 nm, although they reflect only local conformational changes, we actually monitored the global denaturation event.

A comparison of model-dependent $(\Delta H_{VH}^\circ)_{DSC}$ and model-independent $(\Delta H_d^\circ)_{DSC}$ values provides some insight into the nature of the transition to which they refer *(21, 34)*. If they are equal within the experimental error, as in the case of thermal unfolding of EqTxII in pure aqueous solutions at pH 5.5−6.0 and in buffer at pH 3.5 (Table 1), then the observed transition proceeds in a two-state manner, i.e., the concentration of intermediates between the native and the denatured state is negligibly small. On the other hand, if an inequality of the van't Hoff and calorimetrically determined enthalpies of transition is observed, as with EqTxII at low pH, then the melting of the protein molecules cannot be considered as an "all or none" process. A possible cause of the observed $(\Delta H_{VH}^\circ)_{DSC} > (\Delta H_d^\circ)_{DSC}$ for EqTxII at pH 2.0 and 3.0 could be that at low pH the initial state of the protein is already partially denatured. In that case, the measured DSC heat effect would not include the contribution to the heat of transition that results from the pH-induced transition from the initial low-temperature state at pH 5.5−6.0 to the initial low-temperature state at pH 2.0. The corresponding van't Hoff enthalpy of transition, however, calculated from the UV, DSC, or CD melting curves, assumes that the protein undergoes a full native to denatured state transition. Therefore, the approximation of the derivative $(\delta f_D/\delta T)$ used in eqs 4 and 5 will be overestimated, and consequently, the calculated van't Hoff enthalpies of transition will appear larger than the measured $(\Delta H_d^\circ)_{DSC}$ values. Such explanation seems to be in-line with our CD results which definitely show that at pH 2.0 the EqTxII tertiary structure is partially destroyed already at 0 °C.

Experimental determination of $(\Delta H_d^\circ)_{DSC}$, T_d^{DSC}, and the difference in standard heat capacities between the protein's denatured and native state, ΔC_p°, allows us to calculate the temperature dependence of the standard enthalpy, ΔH_d°, standard entropy, ΔS_d°, and standard Gibbs free energy of denaturation, ΔG_d°. Assuming that in the temperature range between 20 and 80 °C, ΔC_P° is constant and independent of the media in which the EqTxII conformational transitions take place and providing that an aggregation of the unfolded protein molecules at higher temperatures does not occur, one obtains *(22, 35)*

$$\Delta H_d^\circ(T) = (\Delta H_{T_d}^\circ)_{DSC} - \int_T^{T_d} \Delta C_P^\circ \, dT = (\Delta H_{T_d}^\circ)_{DSC} - \Delta C_p^\circ(T_d - T) \qquad (6)$$

$$\Delta S_d^\circ(T) = \frac{(\Delta H_{T_d}^\circ)_{DSC}}{T_d} - \int_T^{T_d} \frac{\Delta C_P^\circ}{T} \, dT = \frac{(\Delta H_{T_d}^\circ)_{DSC}}{T_d} - \Delta C_p^\circ \ln \frac{T_d}{T} \qquad (7)$$

$$\Delta G_d^\circ(T) = \Delta H_d^\circ(T) - T\Delta S_d^\circ(T) \qquad (8)$$

Due to the difficulties associated with the experimental determination of ΔC_p° with our DSC instrument, a value of 5.8 kJ mol^{-1} K^{-1}, determined by UV spectroscopy, was employed in these calculations (Figure 2). This value, although determined at 10 times lower toxin concentration, is in good agreement with the experimental value of 5.7 kJ mol^{-1} K^{-1}, obtained from the thermal denaturation of EqTxII in pure aqueous solution, measured as a test case in a far more sensitive DSC instrument DASM-4.

The values of ΔH_d°, ΔS_d°, and ΔG_d°, obtained at 20 °C for EqTxII solutions in triple-distilled water and glycine buffers with pH 3.5, 3.0, and 2.0 from eqs 6, 7, and 8, are presented in Table 2. They show that at 20 °C the EqTxII stability increases with increasing pH and that, at all pH values, except at pH 2.0, the enthalpic contribution that favors stability of the native form only slightly prevails over the entropic contribution that favors the denatured form. The unexpected negative values of ΔH_d° and ΔS_d° contributions calculated at 20 °C and pH 2.0 from eqs 6 and 7 are very likely due to an underestimation of the $\Delta H_{T_d DSC}^\circ$ and a corresponding overestimation of the ΔC_p° value used in these calculations. As shown by the near-UV CD spectroscopy the native state of

Table 2: Values of the Stabilization Parameters ΔH_d°, ΔS_d°, and ΔG_d° of EqTxII at 20 °C at Different pH Calculated from DSC Results by Using Eqs 6−8[a]

pH	[b]ΔH_d° (kJ mol^{-1})	[b]ΔS_d° (kJ mol^{-1} K^{-1})	[b]ΔG_d° (kJ mol^{-1})
2.0	−25	−0.10	3.4
3.0	104	0.28	21.5
3.5	128	0.33	30.6
5.5−6.0	175	0.46	41.0

[a] The value of the difference in standard molar heat capacities between the native and denatured state, ΔC_p°, used in all calculations was 5.8 kJ/mol K. [b] Relative error is estimated to be ±10−20%.

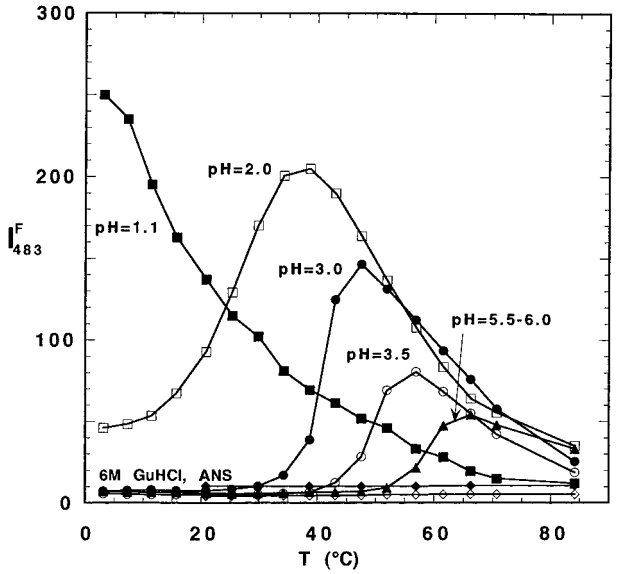

FIGURE 8: ANS fluorescence intensity at 483 nm, I_{483}^F, as a function of temperature in solutions of EqTxII ($c = 0.05$ mg/g$_{solution}$) in glycine buffers at pH 1.1 (■), 2.0 (□), 3.0 (●) and 3.5 (○), in water at pH 5.5−6.0 (▲) in 6 M Gu-HCl (◆), and in any of buffer solutions with no EqTxII present (◇); $c_{ANS} = 0.126$ mg/g$_{solution}$, $\lambda_{exc} = 365$ nm.

EqTxII at 20 °C and pH 2.0 is already partially disrupted. Therefore, its temperature-induced conformational transition should be accompanied by a larger $(\Delta H_{T_d}^\circ)_{DSC}$ and lower ΔC_P° value. Consequently, the ΔH_d° and ΔS_d° contributions calculated from eqs 6 and 7 should be more positive. The ΔG_d° value of 41 ± 10 kJ mol^{-1} determined at 20 °C for EqTxII in pure aqueous solution is in satisfactory agreement with the corresponding ΔG_d° values determined at 25 °C for some other globular proteins of similar size *(36)*. With decreasing pH, the stability of EqTxII, expressed in terms of ΔC_d°, decreases steeply, indicating that at low pH the EqTxII low-temperature initial state may exist in an acid-denatured compact form (Table 2). This result is consistent with our previous findings based on the EqTxII intrinsic fluorescence measurements *(12)*.

ANS Fluorescence. Measurements of the temperature dependence of ANS fluorescence intensity at $\lambda_{em} = 483$ nm, I_{483}^F, show that on lowering pH the peak of the I_{483}^F vs T curve shifts to lower temperatures while its intensity is increased (Figure 8). They also show that at all measured temperatures the fluorescence of ANS in the absence of EqTxII or in the presence of its denatured form in 6 M Gu-HCl is insignificant. Obviously, the measured emission fluorescence results from ANS molecules bound to the protein conformational states that are neither native nor fully

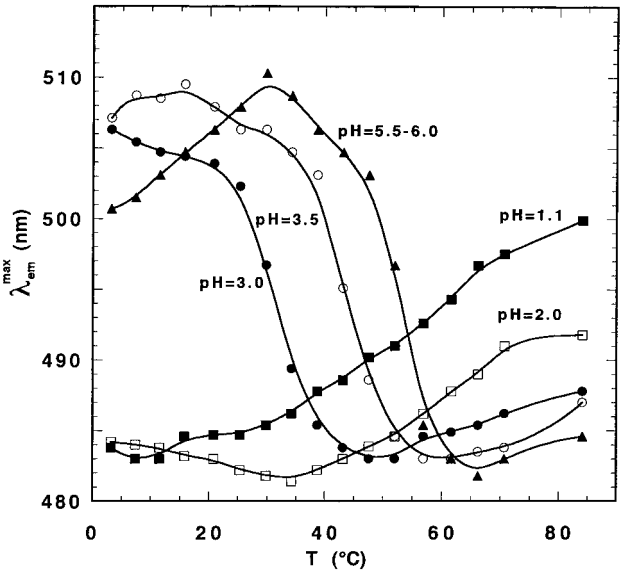

FIGURE 9: Temperature dependence of the wavelength of the ANS fluorescence emission maximum, $(\lambda_{em})_{max}$, in solutions of EqTxII ($c = 0.05$ mg/g$_{solution}$) in glycine buffers at pH 1.1 (■), 2.0 (□), 3.0 (●), and 3.5 (○), and in water at pH 5.5−6.0 (▲), $c_{ANS} = 0.126$ mg/g$_{solution}$, $\lambda_{exc} = 365$ nm.

denatured. A detailed inspection of Figure 8 shows that I_{483}^F maxima appear at temperatures at which the corresponding far- and near-UV CD spectra show a simultaneous collapse of the EqTxII tertiary structure and the transition of its secondary structure from a native β-rich form into a non-native α-helical form (Figure 6). In other words, the EqTxII conformations that exhibit strong binding of ANS seem to contain non-native α-rich secondary structures and no tertiary structure and, thus, show properties of a molten globule state. A presence of α-helical structures as a condition for strong ANS binding to EqTxII intermediates that possess no tertiary structure follows straightforwardly from the comparison of the high-temperature CD spectra of EqTxII and the corresponding ANS fluorescence binding curves (Figures 3−5 and 8). CD spectra show that at high temperatures at each pH EqTxII has only secondary structure whose random coil content increases at the expense of α-helical content. Since the corresponding drop of the ANS fluorescence intensity of about 2 orders of magnitude observed in the relatively narrow temperature interval most probably cannot result only from the thermal quenching or an equally large temperature-induced drop in ANS binding, one can conclude that for ANS binding a molten globule with a significant amount of α-helical secondary structure is required. Furthermore, as shown in Figure 9, the ANS fluorescence emission wavelength at the maximum intensity, λ_{max}, shifts with the thermal unfolding of EqTxII to lower wavelengths. In temperature intervals in which according to UV, CD, DSC, and I_{483}^F measurements, the protein conformational transitions occur, a minimum in the λ_{max} values is observed, and with further increasing of temperature, these peak positions shift back to higher wavelengths. At pH 1.1, only the temperature-induced shift to higher λ_{max} values is observed. Since a blue shift in the emission fluorescence peak of ANS reflects increased hydrophobicity of the medium in which ANS molecules are located, one can, by measuring the emission peak positions of the bound ANS molecules, actually monitor the hydrophobicity of the protein's binding sites. Thus, according to our results, the

optimum hydrophobicity of the EqTxII ANS-binding sites is possessed by the protein intermediate states occurring when the protein undergoes a temperature-induced conformational transition. At pH 1.1, however, at which EqTxII exists at all temperatures up to 60 °C in the molten globule, the highest hydrophobicity of its ANS binding sites is observed at low temperatures ~0 °C.

From Figure 8, one can also see that the ANS fluorescence intensity in the presence of the acid molten globule state at lower temperature is significantly greater than in the presence of the neutral molten globule state at higher temperature. Since ANS fluorescence quantum yield has been shown to depend on the pH of the molten globule *(37)* and will also depend on the temperature, it cannot be used as an absolute measure of the population of intermediate states. Hence, ANS fluorescence peak intensity can only be used as a relative indicator of the molten globule population at a given pH and temperature.

CONCLUDING REMARKS

We have used differential scanning calorimetry in combination with UV and CD spectroscopy and ANS fluorescence to detect and characterize the conformational transitions and individual states of EqTxII as a function of pH and temperature. Our results exhibit the following features: (i) at pH 1.1 in the temperature range from 0 °C to about 60 °C EqTxII exists as a molten globule, lacking the tertiary structure, exhibiting a significant amount of α-helix-rich secondary structure and showing pronounced ANS binding; (ii) in the pH range from 2.0 to 6.0 the heat-induced intermediate states accompanying the protein conformational transition are molten globule states with the same characteristic as at low pH; (iii) at higher temperatures the molten globule states undergo further thermal conformational transitions which are not completed even at 95 °C.

Taken together, these results demonstrate that an equilibrium molten globule state of EqTxII is strongly pH dependent and appears at each pH (1.1−6.0) in a restricted temperature window.

ACKNOWLEDGMENT

We wish to thank Dr. Karl Lohner from the Institute of Biophysics and X-ray Structure Research, Graz, Austria, for performing some DSC experiments on DASM- 4. We would also like to thank Dr. Tigran V. Chalikian, Dr. Jens Völker, and Prof. Dr. Ken J. Breslauer from Rutgers, The State University of New Jersey, Piscataway, NJ, for showing us their results on denaturation studies of α-ctg A before publishing. We are especially grateful to Dr. Jens Völker for critical reading of the manuscript and many helpful suggestions.

REFERENCES

1. van der Goot, F. G., Gonzáles-Mañas, J. M., Lakey, J. H., and Pattus, F. (1991) *Nature 354*, 408−410.
2. Bychkova, V. E., Berni, R., Rossi, G. L., Kutyshenko, V. P., and Ptitsyn, O. B. (1992) *Biochemistry 31*, 7566−7571.
3. Zhao, J.-M., and London, E. (1986) *Proc. Natl. Acad. Sci. U.S.A. 83*, 2002−2006.
4. Ulbrandt, N. D., London, E., and Oliver, D. B. (1992) *J. Biol. Chem. 267*, 15184−15192.
5. Ohgushi, M., and Wada, A. (1983) *FEBS Lett. 164*, 21−24.
6. Dolgikh, D. A., Abaturov, L. K., Bolotina, I. A., Brazhnikov, E. V., Bushuev, V. N., Bychkova, V. E., Gilmanshin, R. I., Lebedev, Yu, O., Semisotnov, G. V., Tiktopulo, E. I., and Ptitsyn, O. B. (1985) *Eur. Biophys. J. 13*, 109−121.
7. Ptitsyn, O. B. (1987) *J. Protein Chem. 6*, 273−293.
8. Eilers, M., Hwang, S., and Schatz, G. (1988) *EMBO J. 7*, 1139−1145.
9. Endo, T., and Schatz, G. (1988) *EMBO J. 7*, 1153−1158.
10. de Jongh, H. H. J., Killian, J. A., and de Kruijff, B. (1992) *Biochemistry 31*, 1636−1643.
11. Belmonte, G., Pederzolli, C., Maček, P., and Menestrina, G. (1993) *J. Membr. Biol. 131*, 11−22.
12. Malavašič, M., Poklar, N., Maček, P., and Vesnaver, G. (1996) *Biochim. Biophys. Acta 1280*, 65−72.
13. Hlodan, R., and Pain, H. R. (1994) *FEBS Lett. 343*, 256−260.
14. Bychkova, V. E., Dujsekina, A. E., Klemin, S. I., Tiktopulo, E. I., Uversky, V. N., and Ptitsyn, O. B. (1996) *Biochemistry 35*, 6058−6063.
15. Maček, P., and Lebez, D. (1988) *Toxicon 26*, 441−451.
16. Shi, L., Palleros, D. R., and Fink, A. L. (1994) *Biochemistry 33*, 7536−7546.
17. Lapanje, S., and Poklar, N. (1989) *Biophys. Chem. 34*, 155−162.
18. Yanary, S., and Bovey, J. (1960) *J. Biol. Chem. 235*, 2818−2826.
19. Campbell, I. D., and Dwek, R. A. (1984) in *Biological Spectroscopy*, pp 61−89, The Benjamine Commings Publishing Comp. Inc., Menlo Park, CA.
20. Donovan, J. W. (1969) *J. Biol. Chem. 244*, 1961−1967.
21. Marky, L. A., and Breslauer, K. J. (1987) *Biopolymers 26*, 1601−1620.
22. Privalov, P. L., and Khechinashvili, N. N. (1974) *J. Mol. Biol. 86*, 665−684.
23. Venyaminov, S. Y., and Yang, J. T. (1996) in *Circular Dichroism and the Conformational Analysis of Biomolecules* (Fasman, G. D., Ed.) pp 69−107, Plenum Press, New York.
24. Provencher, S. W., and Glöckner, J. (1981) *Biochemistry 20*, 33−37.
25. Provencher, S. W. (1982) *Comput. Phys. Commun. 27*, 221−242.
26. Venyaminov, S. Y., Baikalov, I. A., Shen, Z. M., Wu, C.-S. C., and Yang, J. T. (1993) *Anal. Biochem. 214*, 17−24.
27. Belmonte, G., Menestrina, G., Pederzolli, C., Križaj, I., Gubenšek, F., Turk, T., and Maček, P. (1994) *Biochim. Biophys. Acta 1192*, 197−204.
28. Woody, R. W., and Dunker, A. K. in *Circular Dichroism and the Conformational Analysis of Biomolecules* (Fasman, G. D., Ed) pp 109−182, Plenum Press, New York.
29. Goto, Y., and Fink, A. L. (1989) *Biochemistry 28*, 945−952.
30. Ptitsyn, O. B. (1995) *Adv. Protein Chem. 47*, 83−229.
31. Caflisch, A., and Karplus, M. (1995) *J. Mol. Biol. 252*, 672−708.
32. Chalikian, T. V., Völker, J., Anafi, D., and Breslauer, K. (1997) *J. Mol. Biol*. (in press).
33. Hamada, D., Sagawa, S., and Goto Y. (1996) *Nat. Struct. Biol. 3*, 868−873.
34. Lapanje, S. (1978) in *Physicochemical Aspects of Protein Denaturation*, John-Wiley & Sons, New York.
35. Becktel, W. J., and Schellman, J. A, (1987) *Biopolymers 26*, 1859−1877.
36. Privalov, P. L. (1979) *Adv. Protein Chem. 33*, 167−241.
37. Semisotnov, G. V., Rodionova, N. A., Razgulyaev, O. I., Uversky, V. N., Gripas, A. F., and Gilmanshin, R. I. (1991) *Biopolymers 31*, 119−129.

BI971719V